

Journal of Visualized Experiments

Advanced diffusion imaging in the hippocampus of rats with mild traumatic brain injury --Manuscript Draft--

Article Type:	Invited Methods Article - JoVE Produced Video
Manuscript Number:	JoVE60012R2
Full Title:	Advanced diffusion imaging in the hippocampus of rats with mild traumatic brain injury
Keywords:	traumatic brain injury; magnetic resonance imaging; diffusion tensor imaging; preclinical; Rat; hippocampus
Corresponding Author:	Kim Braeckman Universiteit Gent Ghent, BELGIUM
Corresponding Author's Institution:	Universiteit Gent
Corresponding Author E-Mail:	Kim.Braeckman@ugent.be
Order of Authors:	Kim Braeckman Benedicte Descamps Christian Vanhove
Additional Information:	
Question	Response
Please indicate whether this article will be Standard Access or Open Access.	Standard Access (US\$2,400)
Please indicate the city, state/province, and country where this article will be filmed . Please do not use abbreviations.	Ghent, Belgium

TITLE:

Advanced Diffusion Imaging in The Hippocampus of Rats with Mild Traumatic Brain Injury

AUTHORS & AFFILIATIONS:

Kim Braeckman¹, Benedicte Descamps¹, Christian Vanhove¹

¹Infinity lab, Medical Imaging and Signal Processing Group, Ghent University, Ghent, Belgium

Corresponding Author:

Kim Braeckman (kim.braeckman@ugent.be)

Email Addresses of Co-Authors:

Benedicte Descamps (benedicte.descamps@ugent.be)

Christian Vanhove (christian.vanhove@ugent.be)

KEYWORDS:

traumatic brain injury, magnetic resonance imaging, diffusion tensor imaging, preclinical, rat, hippocampus

SUMMARY:

The overall goal of this procedure is to obtain quantitative microstructural information of the hippocampus in a rat with mild traumatic brain injury. This is done using an advanced diffusion-weighted magnetic resonance imaging protocol and region-of-interest based analysis of parametric diffusion maps.

ABSTRACT:

Mild traumatic brain injury (mTBI) is the most common type of acquired brain injury. Since patients with traumatic brain injury show a tremendous variability and heterogeneity (age, gender, type of trauma, other possible pathologies, etc.), animal models play a key role in unraveling factors that are limitations in clinical research. They provide a standardized and controlled setting to investigate the biological mechanisms of injury and repair following TBI. However, not all animal models mimic the diffuse and subtle nature of mTBI effectively. For example, the commonly used controlled cortical impact (CCI) and lateral fluid percussion injury (LFPI) models make use of a craniotomy to expose the brain and induce widespread focal trauma, which are not commonly seen in mTBI. Therefore, these experimental models are not valid to mimic mTBI. Thus, an appropriate model should be used to investigate mTBI. The Marmarou weight drop model for rats induces similar microstructural alterations and cognitive impairments as seen in patients who sustain mild trauma; therefore, this model was selected for this protocol. Conventional computed tomography and magnetic resonance imaging (MRI) scans commonly show no damage following a mild injury, because mTBI induces often only subtle and diffuse injuries. With diffusion weighted MRI, it is possible to investigate microstructural properties of brain tissue, which can provide more insight into the microscopic alterations following mild trauma. Therefore, the goal of this study is to obtain quantitative information of a selected region-of-interest (i.e., hippocampus) to follow up disease

progression after obtaining a mild and diffuse brain injury.

INTRODUCTION:

Traumatic brain injury (TBI) has gained more attention in recent years, as it has become clear that these brain injuries can result in lifelong cognitive, physical, emotional, and social consequences¹. Despite this increasing awareness, mild TBI (mTBI, or concussion) is still often underreported and undiagnosed. MTBI has been referred to as a silent epidemic, and individuals with a history of mTBI show higher rates of substance abuse or psychiatric problems². Several patients with mTBI go undiagnosed every year due to the diffuse and subtle nature of the injuries, which are often not visible on conventional computed tomography (CT) or magnetic resonance imaging (MRI) scans. This lack of radiological evidence of brain injury has led to the development of more advanced imaging techniques such as diffusion MRI, which are more sensitive to microstructural changes³.

Diffusion MRI allows in vivo mapping of the microstructure, and this MRI technique has been used extensively in TBI studies⁴⁻⁶. From the diffusion tensor, fractional anisotropy (FA) and mean diffusivity (MD) are computed to quantify alteration in the microstructural organization following injury. Recent reviews in mTBI patients report increases in FA and decreases in MD following injury, which can be indicative of axonal swelling⁷. Contrary, increases in MD and decreases in FA are also found and have been suggested to underlie disruptions in parenchymal structure following edema formation, axonal degeneration, or fiber misalignment/disruption⁸. These mixed findings can be partially explained by the significant clinical heterogeneity of mTBI caused by different types of impact and severity (e.g., rotation-acceleration, blunt force trauma, blast injury or combination of the former). However, currently there is no clear consensus about the underlying pathology and biological/cellular basis underpinning alterations in the microstructural organization.

Animal models provide a standardized and controlled setting to investigate biological mechanisms of injury and repair following TBI in greater detail. Several experimental models for TBI have been developed and represent different aspects of human TBI (e.g., focal vs. diffuse trauma or trauma caused by rotational forces)^{9,10}. Commonly used animal models include the controlled cortical impact (CCI) and lateral fluid percussion injury (LFPI) models^{11,12}. Although the experimental parameters can be well-controlled, these models make use of a craniotomy to expose the brain. Craniotomies or skull fractures are not commonly seen in mTBI; therefore, these experimental models are not valid to mimic mTBI. The impact acceleration model developed by Marmarou et al.¹³ makes use of a weight that is dropped from a certain height onto the rat's head, which is protected by a helmet. This animal model induces similar microstructural alterations and cognitive impairments as seen in patients who sustain mild trauma. Therefore, this Marmarou weight drop model is appropriate to investigate imaging biomarkers for diffuse mTBI^{14,15}.

This report demonstrates the application of advanced diffusion MRI in an mTBI rat model using the Marmarou weight drop model. First shown is how to induce a mild and diffuse trauma, and

analysis using diffusion tensor imaging (DTI) model is then provided. Specific biological information is obtained with the use of more advanced diffusion models [i.e., diffusion kurtosis imaging (DKI) and white matter tract integrity (WMTI) model]. Specifically, mild trauma is inflicted and microstructural changes are then evaluated in the hippocampus using conventional T2-weighted MRI and an advanced diffusion imaging protocol.

PROTOCOL:

The protocol has been approved by the Animal Ethics Committee at the University of Ghent (ECD 15/44Aanv), and all experiments were conducted in accordance with the guidelines of the European Commission (Directive 2010/63/EU).

1. Animal preparation and helmet attachment

1.1. Weigh a female Wistar H rat (± 250 g or 12 weeks of age) and anesthetize in a small induction chamber filled with a mixture of isoflurane (5%) and O₂ for at least 1 min.

1.2. Inject the rat with 0.05 mg/kg buprenorphine subcutaneously in the neck, return it to the home cage, and allow pre-emptive analgesia for at least 30 min to take an effect.

NOTE: During the 30 min wait, the surgical site can be prepared.

1.3. Place a heating pad kept at 37 °C under the surgical field. Disinfect all surgical instruments and the surgical field with 70% ethanol.

1.4. Place the rat back in the induction chamber and anesthetize the rat until it is non-responsive to a paw or tail pinch.

1.5. Place the rat on the surgical field and insert a catheter in the lateral tail vein. Next, wet the rat's fur with 70% ethanol spray, shave the head, remove excess fur, and disinfect the scalp and the rest of the surgical area with ethanol spray.

1.6. Inject 100 μ L of 2% lidocaine locally in the scalp.

1.7. Make a midline incision to expose the skull, removing any excess membranes with small scissors. Additionally, remove the periosteum by gently rubbing a cotton bud across the skull until the periosteum is no longer present.

1.8. Put one drop of tissue glue on the skull and one on the metallic disc (diameter of 10 mm and 3 mm thickness), which acts as the helmet. Glue the disc approximately one-third before and two-thirds behind the bregma. Allow the glue to dry for 1 min.

2. Induction of traumatic brain injury (TBI)

2.1. Place the rat on the custom-made bed with a foam mattress of certain spring constant (see **Table of Materials**). Position the rat directly under a transparent plastic tube with a 450 g brass weight with the helmet as horizontal as possible. Detach the rat from anesthesia.

2.2. Pull the weight up to 1 m and release when ready. Ensure that a second experimenter is present to move the rat away from the plastic tube immediately after impact to prevent a second impact.

NOTE: The sham injured rats receive the same experimental procedure (steps 1.1–2.7), except for step 2.2.

2.3. Re-attach the rat to the anesthesia and inject 1 mL of physiological solution (0.9% NaCl) via the catheter to reduce the hemodynamic shock.

NOTE: It is possible that the rat briefly stops breathing because of the impact. Gently compress the thorax if the rat does not spontaneously breathe after 2 s to encourage the breathing reflex.

2.4. Remove the helmet by gently pulling it from the skull. Remove any remaining glue from the skull and skin and close the incision with surgical suture. Apply local analgesia gel.

2.5. Place the rat on the bed of the CT scanner. Confirm the correct position using a scout scan. Adjust the field of view to enable imaging of the whole head within one bed position. Administer a general purpose, low dose CT scan to rule out skull fractures.

NOTE: Skull fracture is a criterium for euthanasia.

2.6. Place the rat in a clean cage on a heating pad (37 °C). Monitor the time to regain consciousness. Once the rat is able to sit upright, the rat can be returned to the home cage.

2.7. Administer a second dose of 0.05 mg/kg buprenorphine one day following TBI induction.

3. Diffusion magnetic resonance imaging (MRI)

NOTE: Diffusion-weighted imaging is performed before and 1 day following trauma induction.

3.1. Anesthetize the rat in a small induction chamber filled with a mixture of isoflurane (5%) and O₂. When the rat is non-responsive to a paw or tail pinch reduce the anesthesia to 2% with a flow rate of 500 mL/min. Transfer the animal to the scanner bed in head-first prone position.

3.2. Position the rat in the head holder with the teeth bar and nose cone, delivering the anesthesia, and slide the head forwards until the center of the brain is at the level of the center of the quadrature volume MRI coil. Apply lubricating ointment to the eyes in small amounts to prevent any damage to the cornea. Fixate the head with a small piece of tape to avoid

movement during scanning.

3.3. Place a pressure pad under the thorax of the rat to monitor respiration and cover the rat with a circulating warm water heating blanket and bubble wrap to keep the rat warm. Before the scanning, check the respiratory monitor to ensure that the signal is clear without noise and that the respiratory cycle is consistent. Relocate the pressure pad, if necessary.

NOTE: The respiratory rate should be kept between 1 breath per 1,200–1,700 ms by adjusting the level of anesthesia between 1%–2%.

3.4. Slide the quadrature volume coil over the head. Adjust the tuning and matching capacitors of the coil to the proper frequency and impedance according to the instructions provided by the coil vendor. Advance the scanner bed into the scanner bore to start scanning.

3.5. Obtain a default three-plane scout scan (“tripilot”) to ensure correct positioning.

3.5.1. Load the tripilot sequence into the Scan Control by clicking **New Scan** and selecting the tripilot sequence from the protocol list. Next, click the **traffic light** button to start the scan.

3.5.2. When the scan is finished, load the scan in the image display and ensure that 1) the head is lying straight and 2) the brain is positioned in the center of the magnet and coil. Adjust the position of the head and/or the scanner bed, if necessary, and acquire a new tripilot scan.

3.6. Adjust the local magnetic field using an automated second-order shimming protocol: load the second-order shim protocol into the Scan Control as described in step 3.5.1. Next, click on the **Acq** tab | **Current Adjustments** | **Method specific adjustment for the Local Field Homogeneity** in the Spectrometer Control Tool window to start automated shimming.

3.7. Load a new T2 Rapid imaging with Refocused Echoes (RARE) sequence into the Scan control as described in step 3.5.1.

3.7.1. Acquire T2 weighted images using the default settings, except for the following parameters:

3.7.2. Open the **Edit Scan** tab and adjust the repetition time (TR) and echo time (TE) to 5,500 ms and 37 ms, respectively. Also, modify the field of view and matrix size to allow for a higher in-plane resolution of 109 μm x 109 μm (default resolution = 156 μm x 156 μm). Make sure that the slice thickness is 600 μm , number of slices is set to 45, and RARE factor is set to 8.

3.7.3. Open the **Geometry editor** and place the slice package in the correct position including the bulbus of the brain and the cerebellum.

3.8. Load three new echo-planar diffusion-weighted spin-echo sequence (DtiEpi) from the **B_DIFFUSION** folder into the Scan Control protocol as described in step 3.5.1.

NOTE: Using three different diffusion “shells”, the diffusion tensor imaging (DTI) model^{4,16}, diffusion kurtosis imaging (DKI) model¹⁷, and white matter tract integrity (WMTI) model¹⁸ can all be estimated. It is recommended to use at least three different b-values, with the highest b-value having a maximum of 3000 s/mm² with at least 15 evenly spaced directions per imaging shell¹⁷.

3.8.1. Acquire diffusion weighted images (DWIs) using default settings, apart from the following settings:

3.8.2. Open the **Edit Scan** tab and adjust the geometrical parameters under the **Geometry** tab. Adjust the field of view and matrix size to 105 x 105 to ensure a resolution of 333 µm x 333 µm.

3.8.3. Set the slice orientation to axial and the number of slices to 25, resulting in a slice thickness of 500 µm and interslice distance of 600 µm. Amend the readout direction into left-right.

3.8.4. Click the **Contrast** tab to adjust the echo time to 24 ms and repetition time to 6,250 ms.

3.8.5. Set the bandwidth to 250,000 Hz and turn the fat suppression on. Adjust the number of averages to one.

3.8.6. Click on the **Research** tab and change the number of averages (EPI segments) to 4.

3.8.7. Click on the **Diffusion** tab within the research tab. Perform this step separately for each of the three diffusion shells.

3.8.7.1. Adjust the number of diffusion directions to 32 for the first shell, 46 for the second shell, and 64 for the third shell.

3.8.7.2. Adjust the gradient directions with custom gradient directions files.

3.8.7.3. Change the number of B0 images to 5 for the first shell, 5 for the second shell, and 7 for the third shell.

3.8.7.4. Adjust the b-value per direction to 800 s/mm² for the first shell, 1500 s/mm² for the second shell, and 2000 s/mm² for the third shell.

NOTE: Adjusting the gradient directions with a custom gradient directions file can be done manually by setting **Enter Diffusion Directions** to yes or automatically by using the DTI_SET_DIRECTIONS macro.

3.8.8. Open the **Geometry editor** and place the field of view between the bulbus and cerebellum containing only the cerebrum to reduce artifact and scan time. Position six

saturation bands of 5 mm outside the brain to reduce artifacts by clicking on **Saturation** and sliding the bands in the preferred position using the scroll bars.

NOTE: The bulbus and cerebellum can be identified based on anatomical landmarks and the three images of the tripilot scan.

3.9. Acquire the imported sequences by clicking on the **traffic light** symbol. Using the settings of the parameters described above, the acquisition time of the T2-RARE scan is 12 min, of the first DWI shell 15 min, of the second DWI shell 21 min and of the third shell 30 min. The total acquisition time is approximately 80 min (on a single receiver channel system).

3.10. At the completion of the scanning protocol, remove the animal from the scanner bed, and place the animal in a clean cage with a heating pad at 37 °C. Return the animal to the home cage when it regains consciousness.

4. Image processing

NOTE: In the following sections, the processing of the diffusion images is described in MRtrix3, ExploreDTI¹⁹ and Amide software²⁰ which are open access toolboxes. However, the preprocessing steps can be performed in other toolboxes (e.g., FSL, MedInria, DTIStudio).

4.1. Transfer the acquired data from the acquisition console by exporting the 2dseq file.

4.2. Convert the 2dseq files (raw DWI files) into the .mif format, which is the standard formatting of MRtrix3, to allow for further preprocessing steps in MRtrix3. Moreover, concatenate the three diffusion shells using the following commands in the shell:

```
convert_braker pdata/1/2dseq ratID_T2.mih (for the T2-weighted images)
```

```
convert_braker pdata/1/2dseq ratID_dwi1.mih (for the first diffusion shell)
```

```
convert_braker pdata/1/2dseq ratID_dwi2.mih (for the second diffusion shell)
```

```
convert_braker pdata/1/2dseq ratID_dwi3.mih (for the third diffusion shell)
```

```
mrcat ratID_dwi1.mif ratID_dwi2.mif ratID_dwi3.mif ratID_dwi.mif
```

4.3. Perform noise correction and Gibbs ringing correction on the DWIs in MRtrix3^{21,22}. Also, convert the corrected DWI images and T2 image to NIFTI format using the following commands:

```
dwidenoise ratID_dwi.mif ratID_dwi_denoised.mif
```

```
mrdegibbs ratID_dwi_denoised.mif ratID_dwi_denoised_gr.mif
```

```
mrconvert ratID_dwi_denoised_gr.mif ratID.nii
```

```
mrconvert ratID_T2.mif ratID_T2.nii
```

4.4. Perform correction for EPI, motion and Eddy current distortions in ExploreDTI:

4.4.1. Convert the NIFTI images to a .mat file by clicking **Calculate DTI*.mat file | Convert raw data to DTI*.mat file**. Change the diffusion tensor estimation to weighed linear and the b-value to NaN. Adjust the voxel size to 0.333 0.333 0.6, number of non-DWI images to 17, number of

DWI images to 142, and matrix size to 105 105 25.

NOTE: By setting the b-value to NaN, ExploreDTI will regard the dataset as a kurtosis data set.

4.4.2. Click on the **Settings** tab to adjust the settings for EPI correction (this is turned off by default). Select **SM/EC/EPI correction, also register to other data?** and click on **Yes, to do the EPI correction (non-rigid)**. Specify the suffix of the anatomical T2 image corresponding to the diffusion data set.

NOTE: ExploreDTI corrects for EPI distortions using image registration between the undistorted anatomical image and the diffusion image.

4.4.3. Click on the **Plugins** tab and select **Correction for subject motion & EC/EPI distortions** and select the preprocessed diffusion data file from step 2.3. Make sure that the T2 image is in the same folder and has the same base as the diffusion data file name (e.g., rat1.nii for the DWI and rat1_T2.nii for the anatomical image). This step will generate a “native” (*native.mat) and “transformed” file (*trafo.mat).

4.5. Calculate the DTI metrics for each rat by clicking **Plugins** and **Export stuff to *.nii** and selecting the parametric maps of the DTI model: fractional anisotropy (FA), mean diffusivity (MD), radial diffusivity (RD), and axial diffusivity (AD; denoted as “Smallest eigenvalue L1”).

4.6. Additionally, export the parametric maps for the kurtosis model (MK, AK, and RK) and WMTI model (AWF, AxEAD, RadEAD and TORT). Processing of the diffusion images will result in 12 parametric maps (**Figure 1, Figure 2, Figure 3**) that can be used for further microstructural analysis.

4.7. Create a mask file for the hippocampus of each rat using MRtrix3.

4.7.1. Load the FA image of the rat in the MRtrix viewer by clicking **Tool** and **ROI editor**.

4.7.2. Create a new ROI by clicking the “+” button and press **Edit** to draw the ROI on each slice that includes the hippocampus (**Figure 4**). To erase unwanted areas from the ROI drawn, press the right mouse button.

4.7.3. When the drawing of the ROI is completed, save the mask image by clicking the **Save** button.

NOTE: This mask file will be a binary NIFTI image file with voxels of value 1 containing the hippocampal tissue, and remaining voxels will have values of 0. To standardize the region of the hippocampus across rats, the parametric maps can be co-registered with a study specific template with predefined regions of interest delineated²³ or a rat brain atlas.

4.8. To extract the diffusion metrics of the hippocampus of the rat, use the created mask file of

step 4.6 and open the Amide software.

4.8.1. Open the parametric maps and mask image of the rat.

4.8.2. To add the ROI of the mask file into Amide, select the mask file image, click **Edit | Add ROI | 3D Isocontour** and click on the ROI displayed in the mask image. Give the ROI a meaningful name and confirm that this volume should only contain voxels having a value of one.

4.8.3. To calculate the mean values of the diffusion metrics in the hippocampus, click **Tools | Calculate ROI Statistics** and indicate the images and ROI that should be included. After clicking **Execute**, another screen will pop up with computed values that can be used for further statistical analysis. This file can either be saved or copied into a preferred data format (e.g., .xlsx or .csv file).

5. Statistical analysis

NOTE: In the following sections, we describe processing of the diffusion images in SPSS Statistics 24; however, the statistical analysis can be performed in other statistical toolboxes.

5.1. Load the data in the wide format in an SPSS *.sav file.

5.2. To test for statistical differences between the two groups for each timepoint (i.e., baseline or 1-day post-injury), click **Analyze | Nonparametric tests | Legacy Dialogs | 2 Independent Samples Tests**. Load the variables that need to be tested and specify the groups (i.e., TBI and sham groups). Indicate the Mann-Whitney U as the test type.

5.3. To test for statistical differences between the 2 time point within each group the data file needs to be split. Go to **Data, Split File** and indicate Compare groups. Next, click on **Analyze, Nonparametric tests, Legacy Dialogs, 2 Related Samples Tests**, load the variables that need to be compared and indicate Wilcoxon as test type.

NOTE: To correct for multiple comparisons, p-values are adjusted for each diffusion model using Bonferroni correction [i.e., p-value divided by the number of parameters compared (DTI 4, DKI 3, and WMTI 4)]. More specifically, $p < 0.0125$ is considered significant for the DTI and WMTI models, and $p < 0.016$ is considered significant for the DKI model.

REPRESENTATIVE RESULTS:

In the study, all TBI rats ($n = 10$) survived the impact and were able to recover from the impact and anesthesia within 15 min after detachment from anesthesia²³. On the CT images, there was no evidence of skull fractures and the T2 images did not show any abnormalities such as bleeding, enlarged ventricles, or edema formation at the contusion site 1 day after trauma (**Figure 5**). Thus, based on these visual inspections of the anatomical images, large focal lesions

were not detected, confirming the diffuse and mild nature of the injury.

The quality of the coregistration (non-rigid) step between the T2 image and diffusion data set (step 4.4) was examined by adding an overlay of the T2 image to the color-encoded FA map (**Figure 6**). Then, the FA, MD, AD, and RD parametric maps were calculated (**Figure 1**) and loaded into the Amide software. Based on the FA map, a ROI including the hippocampal structure was drawn (**Figure 4**). Statistical values of the diffusion metrics were calculated averaged over all voxels within the region of interest and the mean values of each DTI metric were exported for further analysis. Another quality check of the diffusion data can be performed by inspecting the outliers in the DTI metrics. For example, FA values in the hippocampus should be around 0.15; therefore, values of <0.10 (denoting isotropic diffusion) or >0.30 (values are seen in white matter) can be regarded as biologically implausible values. These datapoints should be rejected from further analysis. Also, the mean values for AK, RK, and MK of the diffusion kurtosis model as well as the AWF, AxEAD, RadEAD, and TORT of the WMTI model were calculated (**Figure 2, Figure 3**).

In our study, analysis of the DTI metrics revealed significant increased FA values ($p = 0.007$), and decreased diffusivity values (MD and RD) ($p = 0.007$ and $p = 0.007$, respectively) following impact in the mTBI group (**Figure 7**). These decreases in RD and MD were significantly different from the sham group ($p = 0.005$ and $p = 0.004$, respectively). Diffusion kurtosis metrics showed a significant decrease in RK ($p = 0.005$) following impact but no changes in AK or MK (**Figure 8**). Using the WMTI model, RadEAD ($p = 0.007$) and TORT ($p = 0.007$) displayed a significant decrease and increase, respectively, in the mTBI group 1 day after the impact (**Figure 9C,D**). The values in the sham group did not show any significant changes.

FIGURE AND TABLE LEGENDS:

Figure 1: Representative parametric maps for fractional anisotropy (FA), mean diffusivity (MD), axial diffusivity (AD), and radial diffusivity (RD).

Figure 2: Representative parametric maps for mean kurtosis (MK), axial kurtosis (AK), and radial kurtosis (RK).

Figure 3: Representative parametric maps for axonal water fraction (AWF), axial and radial extra axonal diffusivity (AxEAD, RadEAD), and tortuosity (TORT).

Figure 4: Creating a mask in MRtrix3. A ROI is drawn around the hippocampus on all slices containing the volume of the hippocampus, and the volume is saved as a mask file. This can either be done for each rat individually or by using a study specific template mask file to which each of the parametric maps can be co-registered.

Figure 5: CT and T2 weighted images of a representative mTBI animal 1 day after impact. The CT images (top row) do not show any skull fractures. On the T2-weighted images (bottom row) no bleeding, enlarged ventricles, or edema formation were demonstrated. Of note, edema

formation is clearly visible as a hyperintense area around the wound area from the surgical intervention.

Figure 6: Color encoded FA map of diffusion data set overlaid with the anatomical image after correction for EPI, motion, and Eddy current correction in ExploreDTI. Shown is a bad correction and co-registration on the left and good examples on the right. It should be ensured that the color encoding is correct: left-right direction in red (e.g., corpus callosum), anterior-posterior direction in green, and inferior-superior direction in blue (e.g., cingulum). Additionally, the color encoded FA image should be perfectly aligned with the anatomical image.

Figure 7: Changes in diffusion tensor metrics of hippocampus for sham (n = 10) and mTBI animals (n = 10). Following impact, there was a significant increase in FA (A) and significant decreases in mean diffusivity (B) and radial diffusivity (D) in the mTBI animals (B,D). No significant differences were observed for axial diffusivity (C) in the mTBI rats. The sham animals did not show any significant DTI changes (*p < 0.0125).

Figure 8: Changes in diffusion kurtosis metrics of hippocampus for sham (n = 10) and mTBI animals (n = 10). Following impact, there was a significant decrease in RK (C) of the mTBI animals but no changes in AK (B) or MK (A). The sham animals did not show any changes (*p < 0.0166).

Figure 9: Changes in white matter tract integrity metrics of hippocampus for sham (n = 10) and mTBI animals (n = 10). Following impact, there was a significant decrease in RadEAD (C) and significant increase in TORT (D) of the mTBI animals but no change in AWF or AxEAD (A,B). The sham animals did not show any changes (*p < 0.0125).

DISCUSSION:

Since mTBI often is the result of a diffuse and subtle injury that shows no abnormalities on CT and conventional MRI scans, the evaluation of microstructural damage after a mild trauma remains a challenge. Therefore, more advanced imaging techniques are needed to visualize the full extent of the trauma. The application of diffusion magnetic resonance imaging in TBI research has gained more interest during the last decade, where diffusion tensor imaging is most frequently used⁵. A limitation of the DTI model is the assumption of a Gaussian diffusion process that is not a precise assumption for brain microstructure (consisting of a complex network of axons and cells with membranes acting as barriers), resulting in DTI metrics non-specific to the underlying biological microstructure²⁴. Diffusion kurtosis imaging is an extension of the DTI model and attempts to characterize the degree of non-Gaussian diffusion¹⁷. This may provide additional information about tissue heterogeneity or complexity.

Though, a drawback of DTI and DKI models is that they are only a representation of the diffusion signal, which characterizes the probabilistic water displacement profile but is not specific to microstructure⁶. On the other hand, the white matter tract integrity model based on

the kurtosis tensor is a microstructural mapping technique that incorporates *a priori* biological information (assumptions) into the model¹⁸. It attributes the diffusion signal to tissue compartments and can assess biological attributes more directly. These biophysical models may thus offer new information for describing abnormalities after mTBI and overcome this non-specificity issue⁶. Using these three different models, microstructural alterations and biological processes were able to be visualized following mTBI in more detail, specifically by using the Marmarou weight drop model.

The Marmarou weight drop model is easy to use and requires only minor surgery; however, a second experimenter is recommended to move the rat away from the glass tube immediately after the first impact to avoid a second one. Additionally, it is sometimes required to help the rat regain its breathing reflex following the impact. The rather long MRI protocol, with a total acquisition time of around 80 min, is well-tolerated by both the sham and mTBI rats. Though, during scanning, it is important to monitor breathing cycle and adjust the anesthesia if the animal is sleeping too deeply or lightly. It is also important to keep the animal warm both during and after the acquisition until the rat is fully awake to avoid hypothermia.

In advanced diffusion MRI, movement artifacts should be avoided as much as possible. A simple solution to reduce movement during scanning is to make use of a teeth bar and fixate the head with a small piece of tape or two ear bars, if available. This ensures that the head will not move up and down every time the rat takes a breath.

Using advanced diffusion MRI protocols, the acquired images must pass through several (pre-) processing steps, mostly using different software tools, before they can be used for further analysis. A drawback of using different software tools to process the diffusion-weighted images is that (often) each tool uses its own data format to encode the gradient directions table. MRtrix3 stores the gradient information together with the diffusion weighted image in a .mif file, while ExploreDTI makes use of a separate file (B-matrix) to store the gradient directions. Therefore, it is important to check that the gradient directions are correctly transferred from MRtrix3 to ExploreDTI. This can be done by checking that color encoding is correct on color encoded FA images [i.e., left-right direction in red (e.g., corpus callosum), anterior-posterior direction in green, and inferior-superior direction in blue (e.g., cingulum)]. The color encoded FA images can also be used to check the quality of the non-rigid co-registration process between the diffusion-weighted images and structural T2- weighted images.

Using ExploreDTI, parametric maps were extracted using the DTI, DKI, and WMTI models. The DTI model provided parametric maps for MD, AD, RD, and FA, while the DKI model provides parametric maps for MK, AK, and RK. Although four metrics of the WMTI model were calculated (i.e., AWF, AxEAD, RadEAD, TORT), it was not possible to extract intra-axonal diffusivity (IAD) within ExploreDTI. IAD can be obtained using a MATLAB tool provided by the developers of the WMTI model²⁵. To do so, the diffusion-weighted images and gradient information must be transferred again from ExploreDTI into Matlab. This step is again prone to errors concerning the encoding of gradient information. Additionally, the kurtosis tensor and the WMTI parameters must be estimated and calculated again.

Preprocessing of the acquired images, estimation of the tensors, and calculation of the parametric maps requires a long period of computing time. Corrections for EPI, motion, and eddy current required ~40 min per data set on a server with eight cores and 16 GB RAM. Using a ROI analysis, mean values within the hippocampus were calculated before and 1 day after impact. Changes in the DTI, DKI and WMTI metrics were then quantified in the mTBI group. However, in the DKI metrics and AWF of the WMTI model, large inter-subject variability was observed, which resulted in an unexpected difference in baseline values between the sham and mTBI groups. This is most likely the result of voxels containing biologically implausible values (outliers) within the investigated region and may be filtered out in future studies before calculation of the mean values in Amide.

In conclusion, this protocol demonstrates the feasibility of advanced diffusion MRI for investigating and quantifying microstructural alterations in the hippocampus in a rat model of mTBI. Using three different diffusion models, complementary information can be obtained about the underlying biological processes that contribute to the conditions after mTBI. This represents a step forward in the development of biomarkers for mTBI that may be sensitive enough to identify specific microstructural changes in the early phase after mild impact.

ACKNOWLEDGMENTS:

The authors would like to thank Research Foundation - Flanders (FWO) for supporting this work (Grant number: G027815N).

DISCLOSURES:

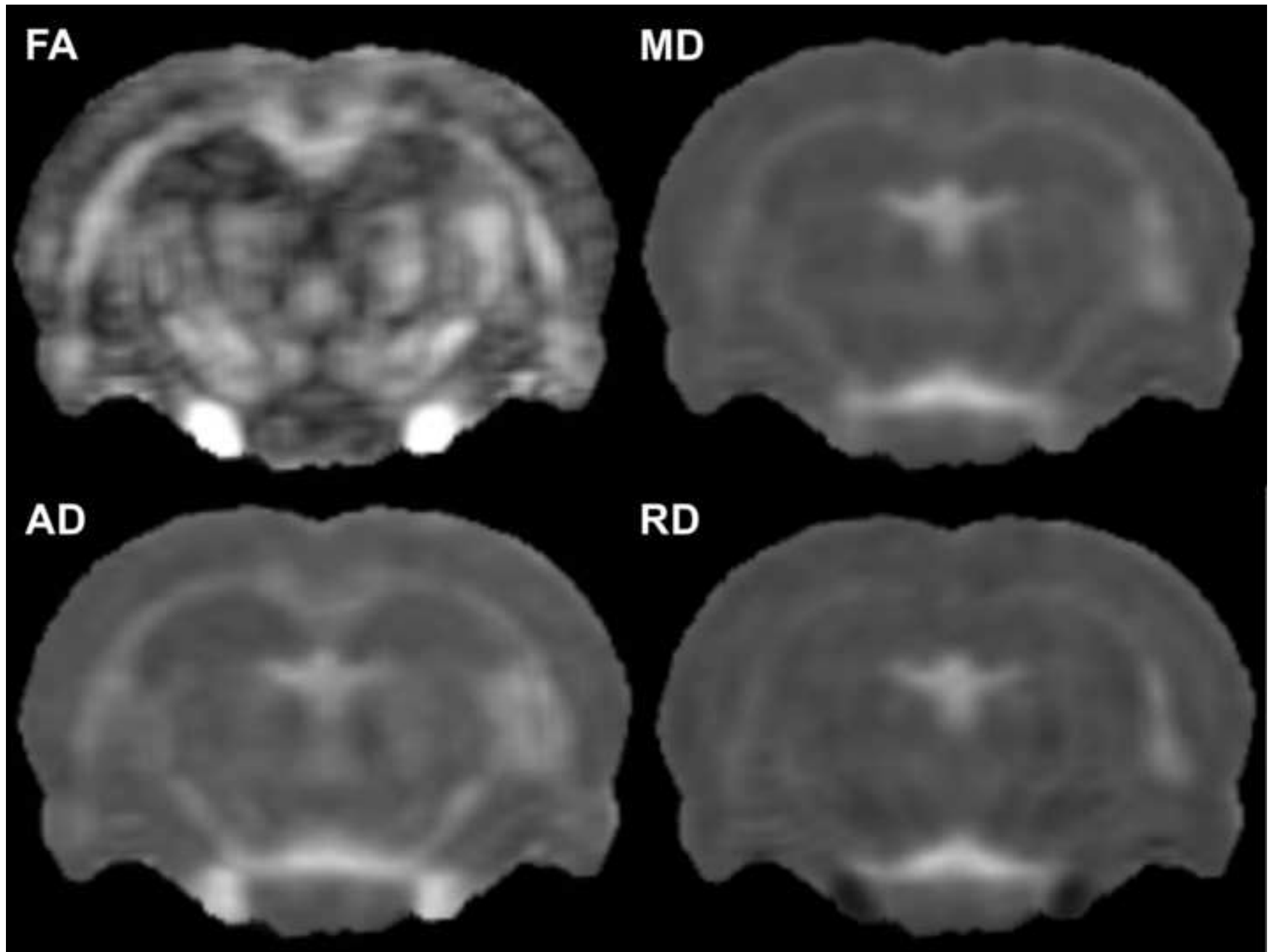
The authors have no conflicts of interest to disclose.

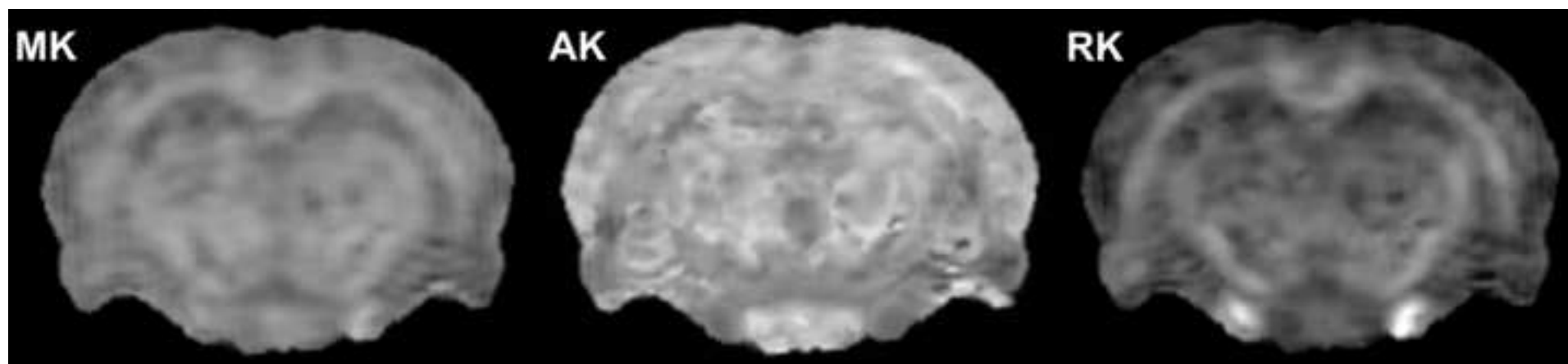
REFERENCES:

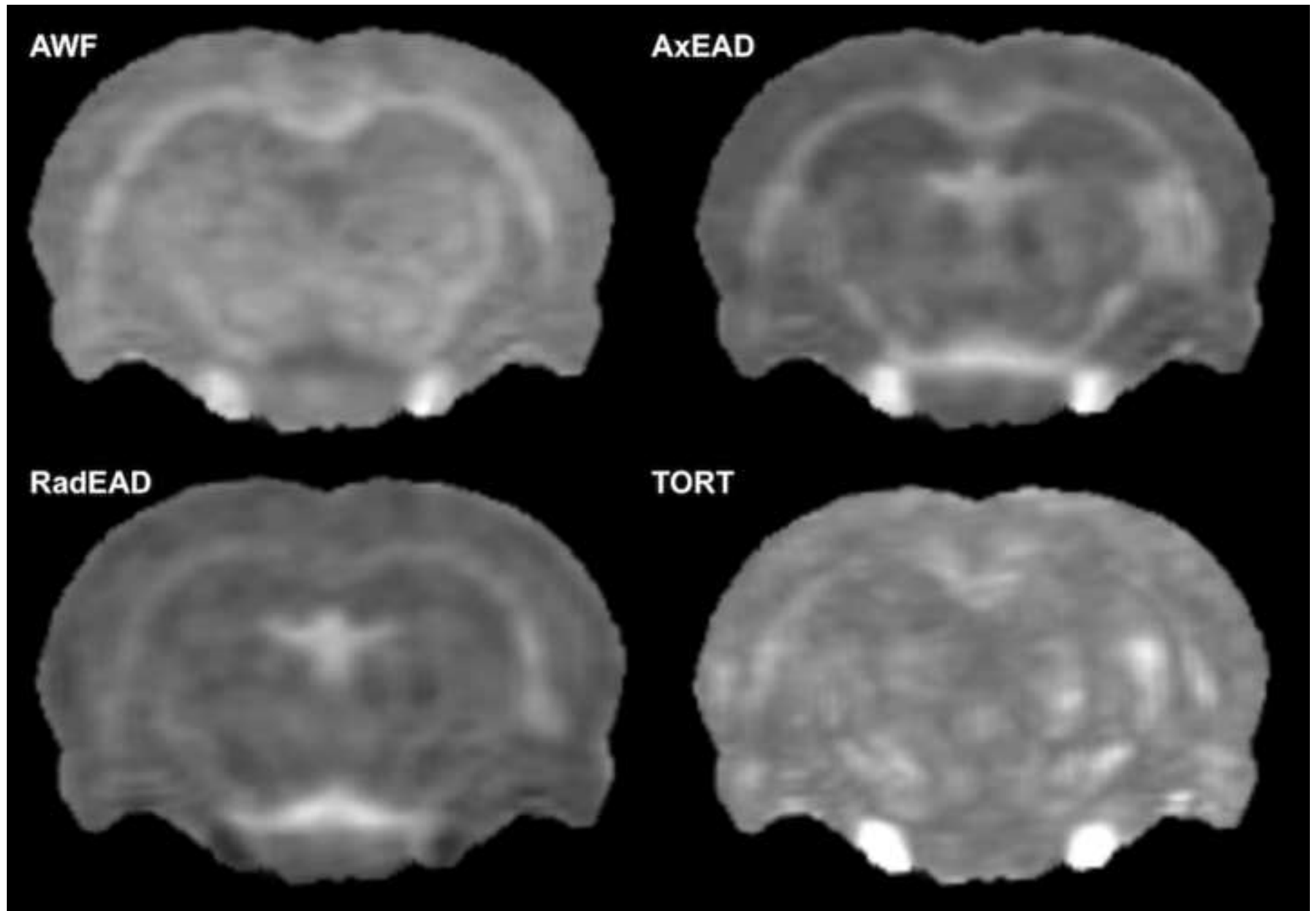
1. Carroll, L. J. et al. Systematic Review of the Prognosis After Mild Traumatic Brain Injury in Adults: Cognitive, Psychiatric, and Mortality Outcomes: Results of the International Collaboration on Mild Traumatic Brain Injury Prognosis. *Archives of Physical Medicine and Rehabilitation*. **95** (3), S152–S173, doi: 10.1016/j.apmr.2013.08.300 (2014).
2. Buck, P. W. Mild Traumatic Brain Injury: A Silent Epidemic in Our Practices. *Health & Social Work*. **36** (4), 299–302, doi: 10.1093/hsw/36.4.299 (2011).
3. Bodanapally, U. K., Sours, C., Zhuo, J., Shanmuganathan, K. Imaging of Traumatic Brain Injury. *Radiologic Clinics of North America*. **53** (4), 695–715, doi: 10.1016/j.rcl.2015.02.011 (2015).
4. Basser, P. J., Mattiello, J., LeBihan, D. MR diffusion tensor spectroscopy and imaging. *Biophysical Journal*. **66** (1), 259–267, doi: 10.1016/S0006-3495(94)80775-1 (1994).
5. Hulkower, M. B., Poliak, D. B., Rosenbaum, S. B., Zimmerman, M. E., Lipton, M. L. A Decade of DTI in Traumatic Brain Injury: 10 Years and 100 Articles Later. *American Journal of Neuroradiology*. **34** (11), 2064–2074, doi: 10.3174/ajnr.A3395 (2013).
6. Hutchinson, E. B., Schwerin, S. C., Avram, A. V., Juliano, S. L., Pierpaoli, C. Diffusion MRI and the detection of alterations following traumatic brain injury. *Journal of Neuroscience Research*. **96** (4), 612–625, doi: 10.1002/jnr.24065 (2018).

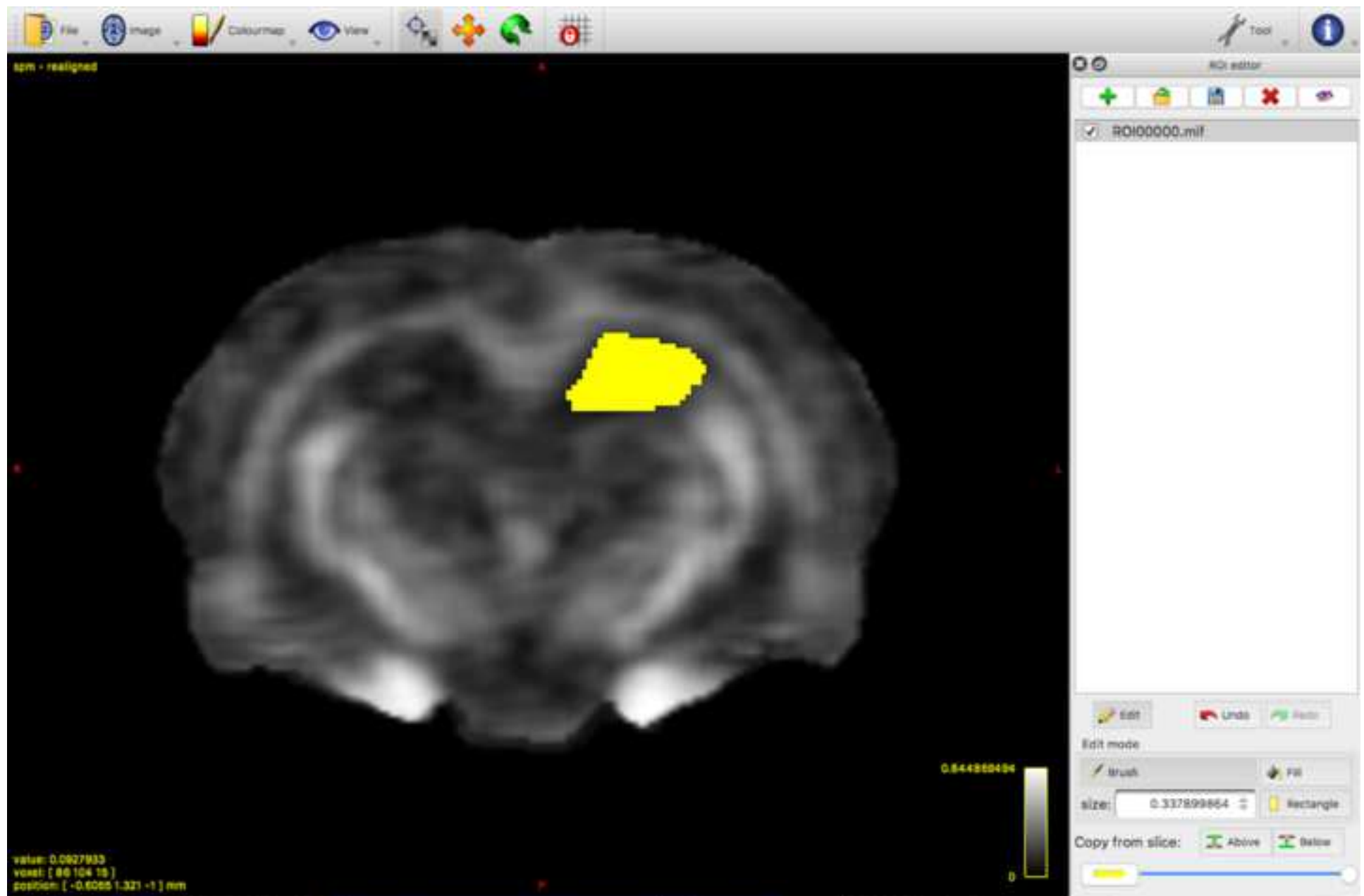
- 573 7. Wallace, E. J., Mathias, J. L., Ward, L. Diffusion tensor imaging changes following mild,
574 moderate and severe adult traumatic brain injury: a meta-analysis. *Brain Imaging and Behavior*.
575 1–15, doi: 10.1007/s11682-018-9823-2 (2018).
- 576 8. Rutgers, D. R. et al. White Matter Abnormalities in Mild Traumatic Brain Injury: A
577 Diffusion Tensor Imaging Study. *American Journal of Neuroradiology*. **29** (3), 514–519, doi:
578 10.3174/ajnr.A0856 (2008).
- 579 9. Bondi, C. O. et al. Found in translation: Understanding the biology and behavior of
580 experimental traumatic brain injury. *Neuroscience & Biobehavioral Reviews*. **58**, 123–146, doi:
581 10.1016/j.neubiorev.2014.12.004 (2015).
- 582 10. Shultz, S. R. et al. The potential for animal models to provide insight into mild traumatic
583 brain injury: Translational challenges and strategies. *Neuroscience & Biobehavioral Reviews*. **76**,
584 396–414, doi: 10.1016/j.neubiorev.2016.09.014 (2017).
- 585 11. Osier, N. D., Dixon, C. E. The Controlled Cortical Impact Model: Applications,
586 Considerations for Researchers, and Future Directions. *Frontiers in Neurology*. **7** (AUG), doi:
587 10.3389/fneur.2016.00134 (2016).
- 588 12. Lyeth, B. G. Historical Review of the Fluid-Perfusion TBI Model. *Frontiers in Neurology*.
589 **7** (DEC), 1–7, doi: 10.3389/fneur.2016.00217 (2016).
- 590 13. Marmarou, A., Foda, M. A. A. -E., Brink, W. van den, Campbell, J., Kita, H., Demetriadou,
591 K. A new model of diffuse brain injury in rats. *Journal of Neurosurgery*. **80** (2), 291–300, doi:
592 10.3171/jns.1994.80.2.0291 (1994).
- 593 14. Heim, L. R. et al. The Invisibility of Mild Traumatic Brain Injury: Impaired Cognitive
594 Performance as a Silent Symptom. *Journal of Neurotrauma*. **34** (17), 2518–2528, doi:
595 10.1089/neu.2016.4909 (2017).
- 596 15. Zohar, O., Rubovitch, V., Milman, A., Schreiber, S., Pick, C. G. Behavioral consequences
597 of minimal traumatic brain injury in mice. *Acta Neurobiol Exp (Wars)*. **71** (1), 36–45 (2011).
- 598 16. Pierpaoli, C., Basser, P. J. Toward a quantitative assessment of diffusion anisotropy.
599 *Magnetic resonance in medicine : official journal of the Society of Magnetic Resonance in*
600 *Medicine / Society of Magnetic Resonance in Medicine*. **36** (6), 893–906, doi:
601 10.1002/mrm.1910360612 (1996).
- 602 17. Jensen, J. H., Helpert, J. A. MRI quantification of non-Gaussian water diffusion by
603 kurtosis analysis. *NMR in Biomedicine*. **23** (7), 698–710, doi: 10.1002/nbm.1518 (2010).
- 604 18. Fieremans, E., Jens H., Jensen, J. A. H. White matter characterization with diffusional
605 kurtosis imaging. *NeuroImage*. **58**, 177–188 (2011).
- 606 19. Leemans, A. Explore DTI.
- 607 20. Loening, A. M., Gambhir, S. S. AMIDE: A Free Software Tool for Multimodality Medical
608 Image Analysis. *Molecular Imaging*. **2** (3), 131–137, doi: 10.1162/153535003322556877 (2003).
- 609 21. Veraart, J. et al. Denoising of diffusion MRI using random matrix theory. *NeuroImage*.
610 **142**, 394–406, doi: 10.1016/j.neuroimage.2016.08.016 (2016).
- 611 22. Veraart, J., Fieremans, E., Novikov, D. S. Diffusion MRI noise mapping using random
612 matrix theory. *Magnetic Resonance in Medicine*. **76** (5), 1582–1593, doi: 10.1002/mrm.26059
613 (2016).
- 614 23. Braeckman, K. et al. Dynamic changes in hippocampal diffusion and kurtosis metrics
615 following experimental mTBI correlate with glial reactivity. *NeuroImage: Clinical*. **21** (August
616 2018), 101669, doi: 10.1016/j.nicl.2019.101669 (2019).

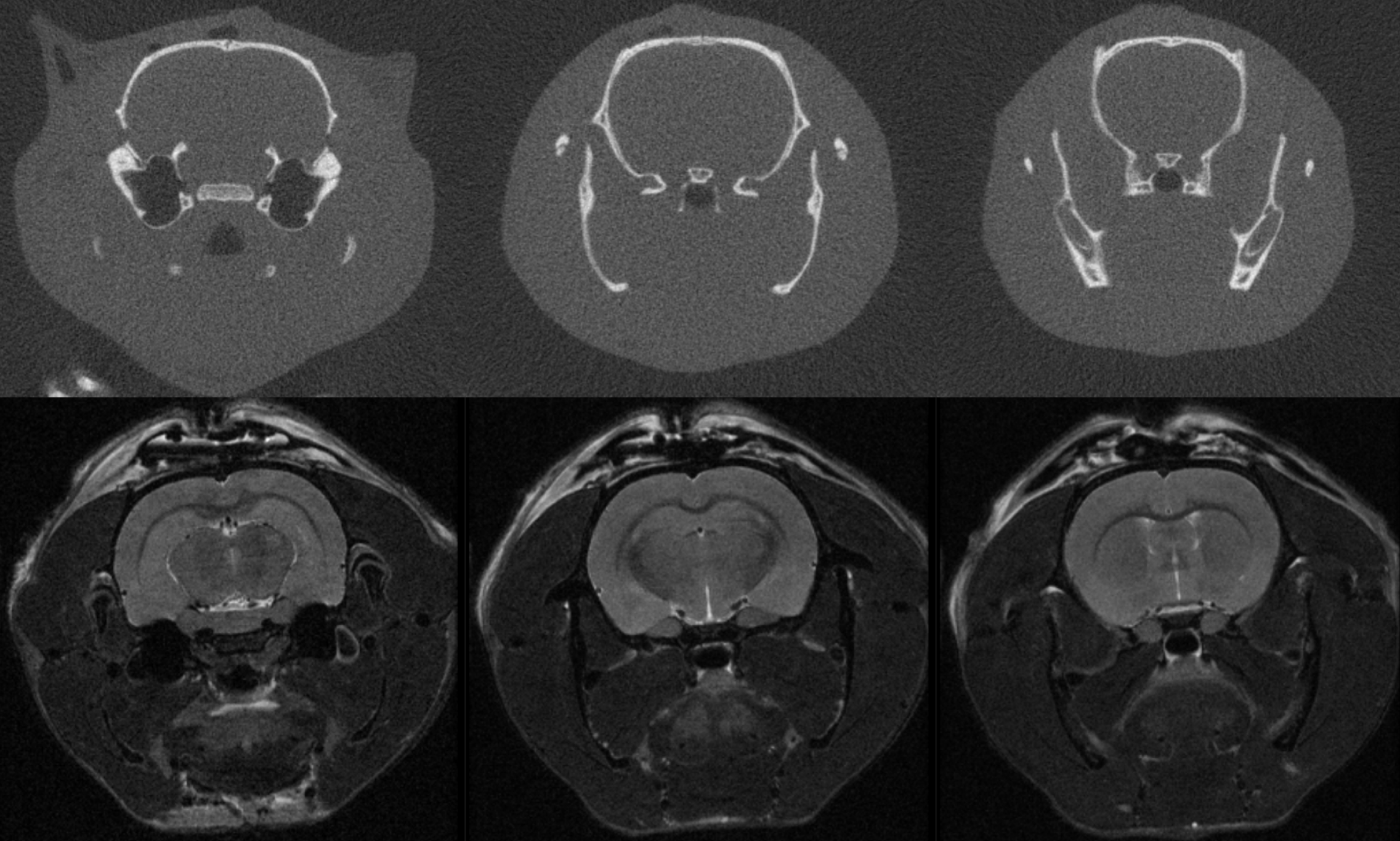
- 617 24. Jones, D. K., Knösche, T. R., Turner, R. White matter integrity, fiber count, and other
618 fallacies: The do's and don'ts of diffusion MRI. *NeuroImage*. **73**, 239–254, doi:
619 10.1016/j.neuroimage.2012.06.081 (2013).
620 25. Matlab code DKI and WMTI model. at <[https://github.com/NYU-DiffusionMRI/Diffusion-](https://github.com/NYU-DiffusionMRI/Diffusion-Kurtosis-Imaging)
621 [Kurtosis-Imaging](https://github.com/NYU-DiffusionMRI/Diffusion-Kurtosis-Imaging)>.
622

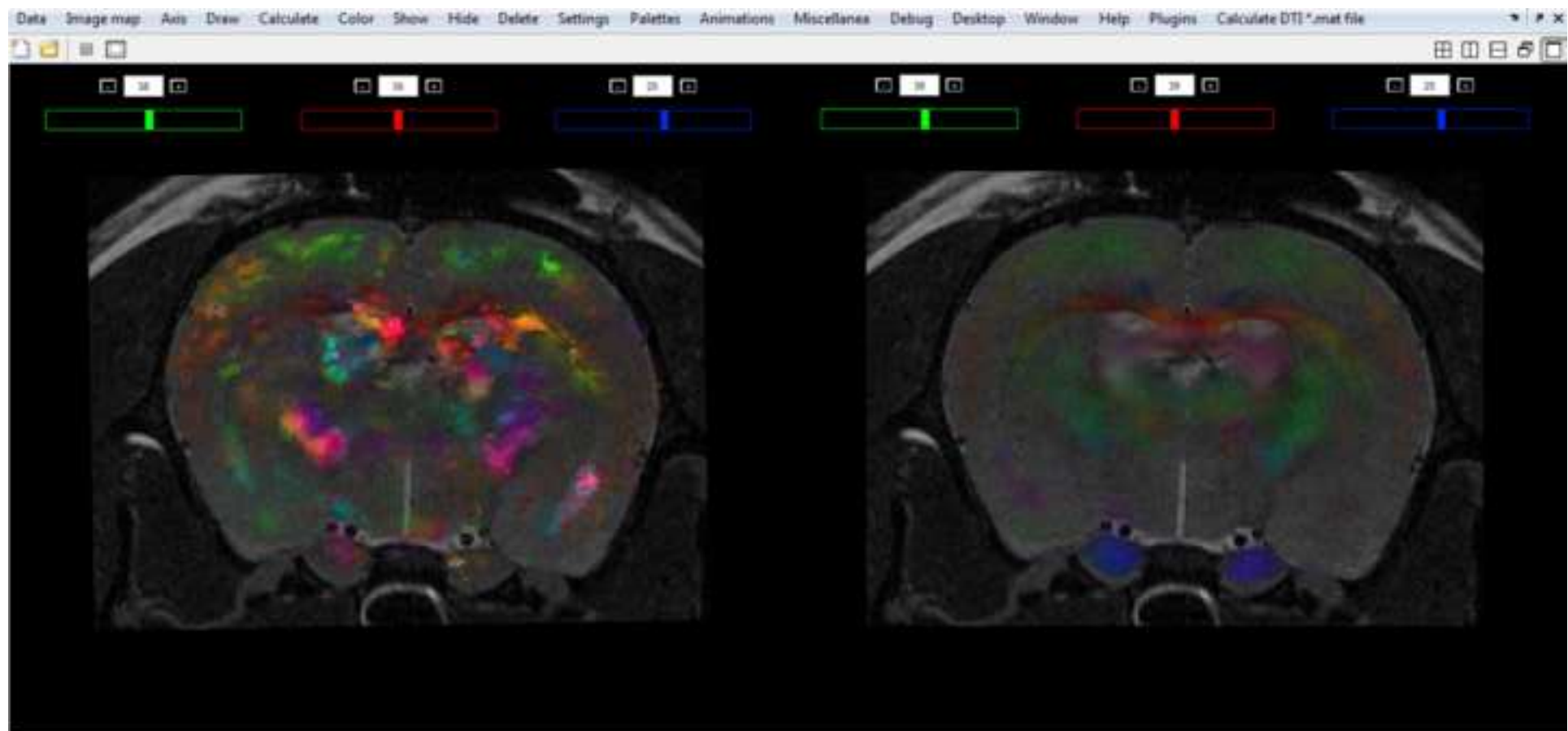


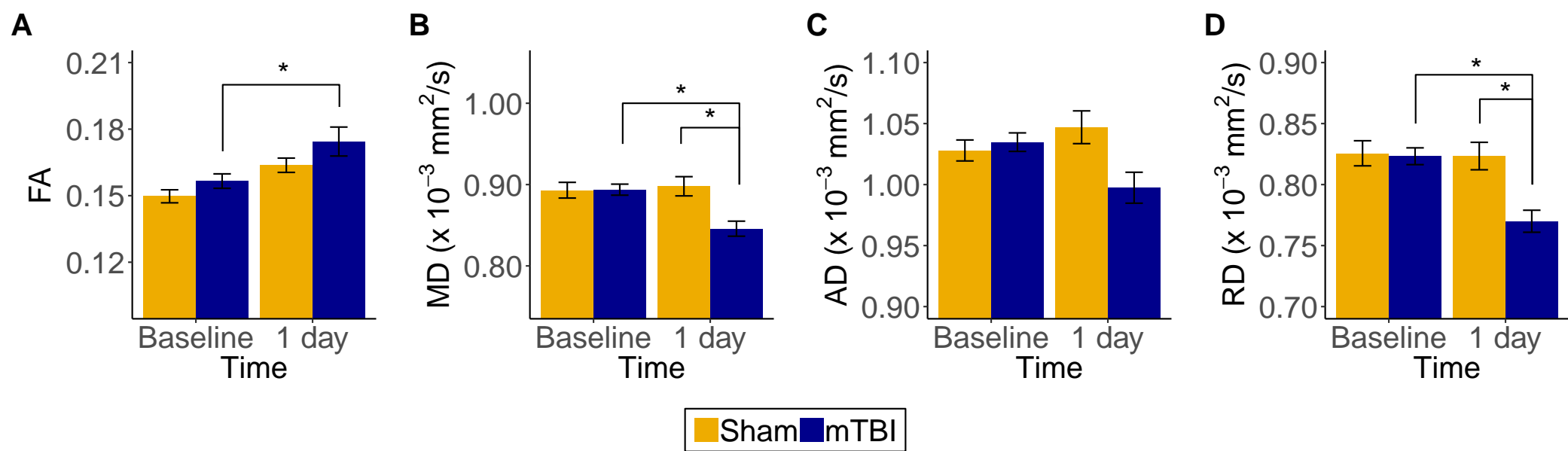




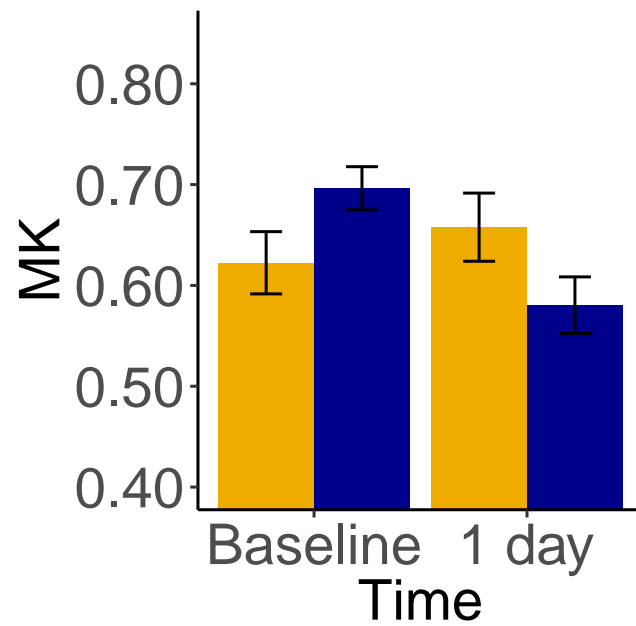




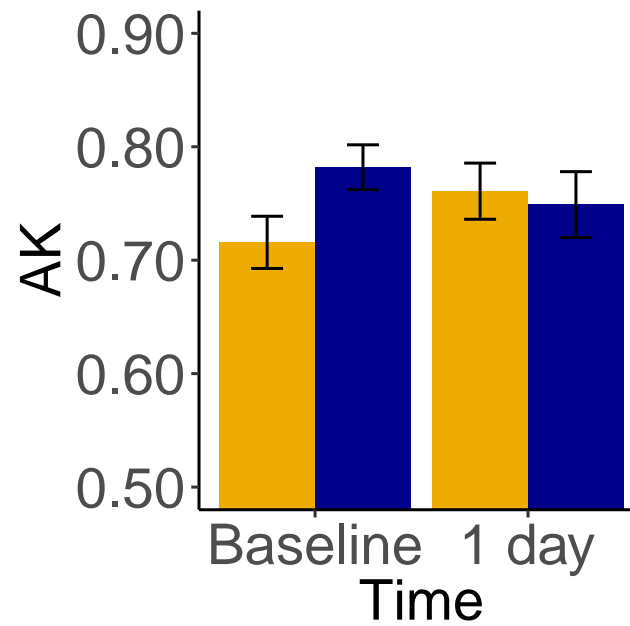




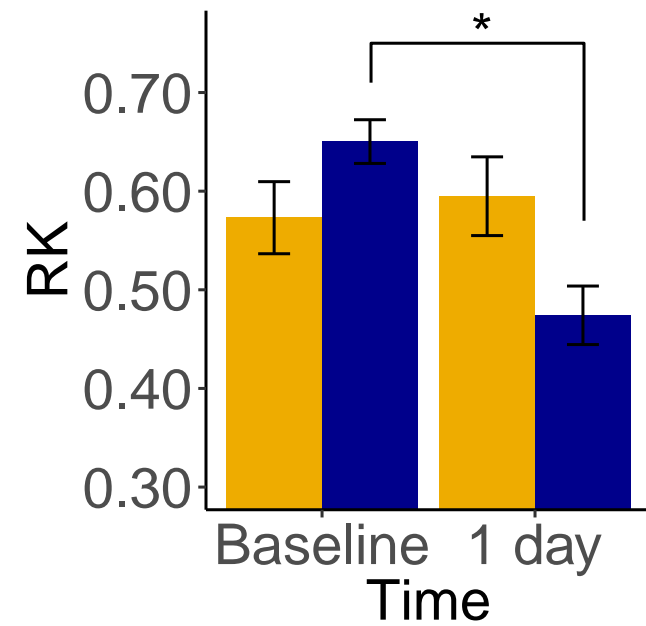
A



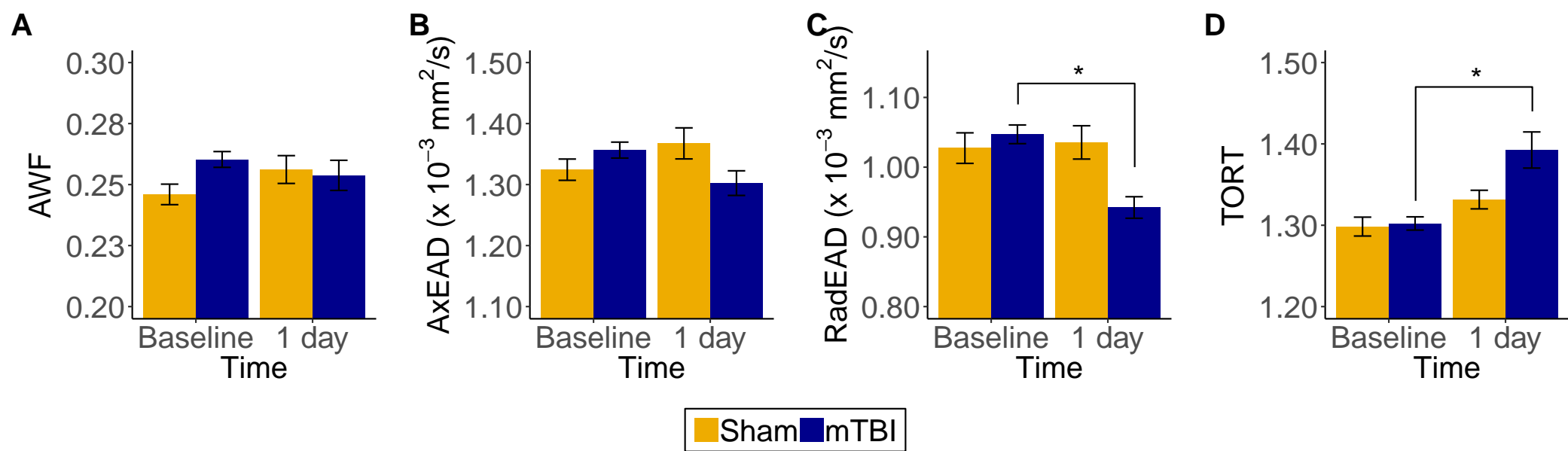
B



C



Sham mTBI



Name of Material/Equipment	Company	Catalog Number	Comments/Description
Induction of trauma			
0.9% NaCl physiologic solution	B Braun	394496	diameter 18mm and 210 mm height
brass weight 450g	custom made	custom made	26G
catheter	Terumo	Versatus-W	FS-3, 4-0, 3/8, 16mm
ethilon II	Ethicon	EH7824	
Matrass	Foam to Size	Type E	
			M1 PMMA XT GOO tube 25x19 mm (inner diameter 19 mm, minimal length of 1.50 m)
Plexiglas tube	ISPA Plastics	416564	
Preclinical CT scanner	Molecubes	X-cube	diameter 10 mm and 3 mm thickness
Steel helmet	custom made	custom made	
Vetbond Tissue Adhesive	3M	1469SB	
Vetergesic (buprenorphin)	EcuPhar	VETERG20	0.05 mg/kg
Xylocaine 2% gel	AstraZeneca	Xylocaine 2%	gel
	Aspen/AstraZeneca		
Xylocaine (lidocaine 2%)	a	Xylocaine 2% gel	100 µl injection
Diffusion MRI			
	Bruker Biospin		ParaVision 5.1 MRI software
Preclinical MRI acquisition software	MRI GmbH	Z400_PV51_CENTOS55	
	Bruker Biospin		
Preclinical MRI scanner	MRI GmbH	PharmaScan 70/16	7T MRI scanner
	Bruker Biospin	RF RES 300 1H 075/040	
Quadrature volume coil	MRI GmbH	QSN TR	Model No: 1P T13161C3
Small animal physiological monitoring unit	Rapid Biomedical	EKGHR02-0571-043C01	Unit for respiratory monitoring
	Thermo Fisher		
Water-based heating unit	Scientific	Haake S 5P	Model No: 1523051

Anaesthesia

Anaesthesia movable unit	Veterenary		
isoflurane: Isoflo	technics		BDO - Medipass, Ijmuiden
	Zoetis	B506	
Oxygen generator	Veterenary		
	technics	7F-3	BDO - Medipass, Ijmuiden

Diffusion image processing

			Medical Imaging Data Examiner Toolbox (Loening AM, Gambhir SS, " AMIDE: A Free Software Tool for Multimodality Medical Image Analysis", Molecular Imaging, 2(3):131-137, 2003)
Amide	http://amide.sourceforge.net	Version 1.0.5.	
			Toolbox for (pre-)processing and analysis of diffusion weighted MR images (Leemans A, Jeurissen B, Sijbers J, and Jones DK. ExploreDTI: a graphical toolbox for processing, analyzing, and visualizing diffusion MR data. In: 17th Annual Meeting of Intl Soc Mag Reson Med, p. 3537, Hawaii, USA, 2009)
ExploreDTI	http://www.explore-dti.com	Version 4.8.6	

MRtrix3

<http://www.mrtrix.org> Version 3.0_RC3-86-g4b523b41

Toolbox for (pre-)processing and analysis of diffusion weighted MR images

ARTICLE AND VIDEO LICENSE AGREEMENT

Title of Article:	Advanced diffusion imaging in the hippocampus of rats with mild traumatic brain injury
Author(s):	Kim Braeckman, Benedicte Descamps, Karen Caeyenberghs, Christian Vanhove

Item 1: The Author elects to have the Materials be made available (as described at <http://www.jove.com/publish>) via:



Standard Access



Open Access

Item 2: Please select one of the following items:



The Author is **NOT** a United States government employee.



The Author is a United States government employee and the Materials were prepared in the course of his or her duties as a United States government employee.



The Author is a United States government employee but the Materials were NOT prepared in the course of his or her duties as a United States government employee.

ARTICLE AND VIDEO LICENSE AGREEMENT

1. **Defined Terms.** As used in this Article and Video License Agreement, the following terms shall have the following meanings: “**Agreement**” means this Article and Video License Agreement; “**Article**” means the article specified on the last page of this Agreement, including any associated materials such as texts, figures, tables, artwork, abstracts, or summaries contained therein; “**Author**” means the author who is a signatory to this Agreement; “**Collective Work**” means a work, such as a periodical issue, anthology or encyclopedia, in which the Materials in their entirety in unmodified form, along with a number of other contributions, constituting separate and independent works in themselves, are assembled into a collective whole; “**CRC License**” means the Creative Commons Attribution-Non Commercial-No Derivs 3.0 Unported Agreement, the terms and conditions of which can be found at: <http://creativecommons.org/licenses/by-nc-nd/3.0/legalcode>; “**Derivative Work**” means a work based upon the Materials or upon the Materials and other pre-existing works, such as a translation, musical arrangement, dramatization, fictionalization, motion picture version, sound recording, art reproduction, abridgment, condensation, or any other form in which the Materials may be recast, transformed, or adapted; “**Institution**” means the institution, listed on the last page of this Agreement, by which the Author was employed at the time of the creation of the Materials; “**JoVE**” means MyJoVE Corporation, a Massachusetts corporation and the publisher of The Journal of Visualized Experiments; “**Materials**” means the Article and / or the Video; “**Parties**” means the Author and JoVE; “**Video**” means any video(s) made by the Author, alone or in conjunction with any other parties, or by JoVE or its affiliates or agents, individually or in collaboration with the Author or any other parties, incorporating all or any portion

of the Article, and in which the Author may or may not appear.

2. **Background.** The Author, who is the author of the Article, in order to ensure the dissemination and protection of the Article, desires to have the JoVE publish the Article and create and transmit videos based on the Article. In furtherance of such goals, the Parties desire to memorialize in this Agreement the respective rights of each Party in and to the Article and the Video.

3. **Grant of Rights in Article.** In consideration of JoVE agreeing to publish the Article, the Author hereby grants to JoVE, subject to **Sections 4** and **7** below, the exclusive, royalty-free, perpetual (for the full term of copyright in the Article, including any extensions thereto) license (a) to publish, reproduce, distribute, display and store the Article in all forms, formats and media whether now known or hereafter developed (including without limitation in print, digital and electronic form) throughout the world, (b) to translate the Article into other languages, create adaptations, summaries or extracts of the Article or other Derivative Works (including, without limitation, the Video) or Collective Works based on all or any portion of the Article and exercise all of the rights set forth in (a) above in such translations, adaptations, summaries, extracts, Derivative Works or Collective Works and (c) to license others to do any or all of the above. The foregoing rights may be exercised in all media and formats, whether now known or hereafter devised, and include the right to make such modifications as are technically necessary to exercise the rights in other media and formats. If the “Open Access” box has been checked in **Item 1** above, JoVE and the Author hereby grant to the public all such rights in the Article as provided in, but subject to all limitations and requirements set forth in, the CRC License.

ARTICLE AND VIDEO LICENSE AGREEMENT

4. **Retention of Rights in Article.** Notwithstanding the exclusive license granted to JoVE in **Section 3** above, the Author shall, with respect to the Article, retain the non-exclusive right to use all or part of the Article for the non-commercial purpose of giving lectures, presentations or teaching classes, and to post a copy of the Article on the Institution's website or the Author's personal website, in each case provided that a link to the Article on the JoVE website is provided and notice of JoVE's copyright in the Article is included. All non-copyright intellectual property rights in and to the Article, such as patent rights, shall remain with the Author.

5. **Grant of Rights in Video – Standard Access.** This **Section 5** applies if the "Standard Access" box has been checked in **Item 1** above or if no box has been checked in **Item 1** above. In consideration of JoVE agreeing to produce, display or otherwise assist with the Video, the Author hereby acknowledges and agrees that, Subject to **Section 7** below, JoVE is and shall be the sole and exclusive owner of all rights of any nature, including, without limitation, all copyrights, in and to the Video. To the extent that, by law, the Author is deemed, now or at any time in the future, to have any rights of any nature in or to the Video, the Author hereby disclaims all such rights and transfers all such rights to JoVE.

6. **Grant of Rights in Video – Open Access.** This **Section 6** applies only if the "Open Access" box has been checked in **Item 1** above. In consideration of JoVE agreeing to produce, display or otherwise assist with the Video, the Author hereby grants to JoVE, subject to **Section 7** below, the exclusive, royalty-free, perpetual (for the full term of copyright in the Article, including any extensions thereto) license (a) to publish, reproduce, distribute, display and store the Video in all forms, formats and media whether now known or hereafter developed (including without limitation in print, digital and electronic form) throughout the world, (b) to translate the Video into other languages, create adaptations, summaries or extracts of the Video or other Derivative Works or Collective Works based on all or any portion of the Video and exercise all of the rights set forth in (a) above in such translations, adaptations, summaries, extracts, Derivative Works or Collective Works and (c) to license others to do any or all of the above. The foregoing rights may be exercised in all media and formats, whether now known or hereafter devised, and include the right to make such modifications as are technically necessary to exercise the rights in other media and formats. For any Video to which this **Section 6** is applicable, JoVE and the Author hereby grant to the public all such rights in the Video as provided in, but subject to all limitations and requirements set forth in, the CRC License.

7. **Government Employees.** If the Author is a United States government employee and the Article was prepared in the course of his or her duties as a United States government employee, as indicated in **Item 2** above, and any of the licenses or grants granted by the Author hereunder exceed the scope of the 17 U.S.C. 403, then the rights granted hereunder shall be limited to the maximum

rights permitted under such statute. In such case, all provisions contained herein that are not in conflict with such statute shall remain in full force and effect, and all provisions contained herein that do so conflict shall be deemed to be amended so as to provide to JoVE the maximum rights permissible within such statute.

8. **Protection of the Work.** The Author(s) authorize JoVE to take steps in the Author(s) name and on their behalf if JoVE believes some third party could be infringing or might infringe the copyright of either the Author's Article and/or Video.

9. **Likeness, Privacy, Personality.** The Author hereby grants JoVE the right to use the Author's name, voice, likeness, picture, photograph, image, biography and performance in any way, commercial or otherwise, in connection with the Materials and the sale, promotion and distribution thereof. The Author hereby waives any and all rights he or she may have, relating to his or her appearance in the Video or otherwise relating to the Materials, under all applicable privacy, likeness, personality or similar laws.

10. **Author Warranties.** The Author represents and warrants that the Article is original, that it has not been published, that the copyright interest is owned by the Author (or, if more than one author is listed at the beginning of this Agreement, by such authors collectively) and has not been assigned, licensed, or otherwise transferred to any other party. The Author represents and warrants that the author(s) listed at the top of this Agreement are the only authors of the Materials. If more than one author is listed at the top of this Agreement and if any such author has not entered into a separate Article and Video License Agreement with JoVE relating to the Materials, the Author represents and warrants that the Author has been authorized by each of the other such authors to execute this Agreement on his or her behalf and to bind him or her with respect to the terms of this Agreement as if each of them had been a party hereto as an Author. The Author warrants that the use, reproduction, distribution, public or private performance or display, and/or modification of all or any portion of the Materials does not and will not violate, infringe and/or misappropriate the patent, trademark, intellectual property or other rights of any third party. The Author represents and warrants that it has and will continue to comply with all government, institutional and other regulations, including, without limitation all institutional, laboratory, hospital, ethical, human and animal treatment, privacy, and all other rules, regulations, laws, procedures or guidelines, applicable to the Materials, and that all research involving human and animal subjects has been approved by the Author's relevant institutional review board.

11. **JoVE Discretion.** If the Author requests the assistance of JoVE in producing the Video in the Author's facility, the Author shall ensure that the presence of JoVE employees, agents or independent contractors is in accordance with the relevant regulations of the Author's institution. If more than one author is listed at the beginning of this Agreement, JoVE may, in its sole

ARTICLE AND VIDEO LICENSE AGREEMENT

discretion, elect not take any action with respect to the Article until such time as it has received complete, executed Article and Video License Agreements from each such author. JoVE reserves the right, in its absolute and sole discretion and without giving any reason therefore, to accept or decline any work submitted to JoVE. JoVE and its employees, agents and independent contractors shall have full, unfettered access to the facilities of the Author or of the Author's institution as necessary to make the Video, whether actually published or not. JoVE has sole discretion as to the method of making and publishing the Materials, including, without limitation, to all decisions regarding editing, lighting, filming, timing of publication, if any, length, quality, content and the like.

12. **Indemnification.** The Author agrees to indemnify JoVE and/or its successors and assigns from and against any and all claims, costs, and expenses, including attorney's fees, arising out of any breach of any warranty or other representations contained herein. The Author further agrees to indemnify and hold harmless JoVE from and against any and all claims, costs, and expenses, including attorney's fees, resulting from the breach by the Author of any representation or warranty contained herein or from allegations or instances of violation of intellectual property rights, damage to the Author's or the Author's institution's facilities, fraud, libel, defamation, research, equipment, experiments, property damage, personal injury, violations of institutional, laboratory, hospital, ethical, human and animal treatment, privacy or other rules, regulations, laws, procedures or guidelines, liabilities and other losses or damages related in any way to the submission of work to JoVE, making of videos by JoVE, or publication in JoVE or elsewhere by JoVE. The Author shall be responsible for, and shall hold JoVE harmless from, damages caused by lack of sterilization, lack of cleanliness or by contamination due to

the making of a video by JoVE its employees, agents or independent contractors. All sterilization, cleanliness or decontamination procedures shall be solely the responsibility of the Author and shall be undertaken at the Author's expense. All indemnifications provided herein shall include JoVE's attorney's fees and costs related to said losses or damages. Such indemnification and holding harmless shall include such losses or damages incurred by, or in connection with, acts or omissions of JoVE, its employees, agents or independent contractors.

13. **Fees.** To cover the cost incurred for publication, JoVE must receive payment before production and publication the Materials. Payment is due in 21 days of invoice. Should the Materials not be published due to an editorial or production decision, these funds will be returned to the Author. Withdrawal by the Author of any submitted Materials after final peer review approval will result in a US\$1,200 fee to cover pre-production expenses incurred by JoVE. If payment is not received by the completion of filming, production and publication of the Materials will be suspended until payment is received.

14. **Transfer, Governing Law.** This Agreement may be assigned by JoVE and shall inure to the benefits of any of JoVE's successors and assignees. This Agreement shall be governed and construed by the internal laws of the Commonwealth of Massachusetts without giving effect to any conflict of law provision thereunder. This Agreement may be executed in counterparts, each of which shall be deemed an original, but all of which together shall be deemed to be one and the same agreement. A signed copy of this Agreement delivered by facsimile, e-mail or other means of electronic transmission shall be deemed to have the same legal effect as delivery of an original signed copy of this Agreement.

A signed copy of this document must be sent with all new submissions. Only one Agreement is required per submission.

CORRESPONDING AUTHOR

Name:

Kim Braeckman

Department:

Infinity Lab - Medical Imaging and Processing Group

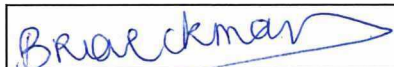
Institution:

Ghent University

Title:

M.Sc.

Signature:



Date:

18/03/2019

Please submit a **signed** and **dated** copy of this license by one of the following three methods:

1. Upload an electronic version on the JoVE submission site
2. Fax the document to +1.866.381.2236
3. Mail the document to JoVE / Attn: JoVE Editorial / 1 Alewife Center #200 / Cambridge, MA 02140

Vineeta Bajaj, Ph.D.
Review Editor
Journal of Visualized Experiments

Kim Braeckman
PhD student

kim.braeckman@ugent.be
InfinityLab, IBiTech-Medisip
Faculty of Engineering Sciences and Architecture
Ghent University
Blok B-5 (Ingang 36),
Corneel Heymanslaan 10,
9000 Gent
BELGIUM

DATE

30 April 2019

Ref.: Manuscript ID JoVE60012 entitled “Advanced diffusion imaging in the hippocampus of rats with mild traumatic brain injury”

Dear Editor,

Thank you again for handling our manuscript. We have fully proof read the article and adjusted the remarks in the document. Below, you can find the feedback to specific comments. Please find in attachment the resubmitted version of the original manuscript with track changes. We would like to state that the figures in the manuscript are entirely new and do not fall under copyright. The authors would like to thank you again for taking our work under consideration for publication in JoVE.

Kind regards,
Kim Braeckman

Editor's comments:

1. The editor has formatted the manuscript to match the journal's style. Please retain the same.
2. Please address specific comments marked in the manuscript.
3. Once done please highlight 2.75 pages of the protocol including headings and spacings. Please highlight complete sentences.
4. Please do not use commercial terms in the manuscript. All commercial terms can be moved to the table of materials.
4. Please proofread the manuscript well before submitting.

Response: The manuscript has been formatted to match the journal's style, specific comments have been addressed (see track changes) and the highlighted section has been adapted. Commercial terms have been moved to the Table of Materials.